Analysis of Quasi-Dynamic Ordinary Differential Equations and the Quasi-Dynamic Replicator

Christopher Griffin* Libo Jiang † Rongling Wu‡

July 2, 2020

Abstract

We study the mathematical properties of the quasi-dynamic ordinary differential equations defined empirically in [Chen et al. An omnidirectional visualization model of personalized gene regulatory networks, *npj Systems Biology and Applications*, 5(1):38, 2019]. In particular, we show how the allometric scaling mentioned in that work emerges naturally from the generalized Lotka-Volterra model under the quasi-dynamic ordinary differential equations paradigm. We then define and study the proportional quasi-dynamic ordinary differential equations and discuss the relationship of this equation system to both the classical and discrete time replicator dynamics. We prove asymptotic properties of these systems for large and small populations and show that there exist populations for which the proportion of the population varies cyclically as a function of total logarithmic population size.

1 Introduction

Dynamic analysis of gene and/or microbiota data requires access to high fidelity longitudinal data that are often not available. Especially in human subjects, each sample in time requires an invasive procedure that may not be possible from a practical or ethical standpoint. Consequently, the dynamic analysis of microbiota data is frequently difficult and relies on temporally sparse data sets. In contrast, many of these data sets are complete in the sense that they have many samples from a (large) population. In [1] it is noted that these data can be used more efficiently by making a change from the time domain to the *niche index* [2–5] domain. By this, we mean one can characterize the interactions of microbiota in the context of the net population within the environment. This is the the so-called *niche index* characterizing the overall fitness of all populations. When multiple hosts have been sampled (even if infrequently), the result is a dense sample of niche index values from which dynamics can be inferred. Differential equation originally written in time can be rephrased in terms of niche index. [1] calls these equations *quasi-dynamic ordinary differential equations* (qdODE).

In this paper, we use the definition of niche index provided in [1] and use it in the context of the classical generalized Lotka-Volterra equations to explore the mathematical properties of quasi-dynamic ordinary differential equations. We show that these qdODE have special structure and that they admit allometric scaling naturally. This was observed empirically in [1]. We then derive a new system of autonomous differential equations that we call the proportional quasi-dynamic ordinary differential equations (pqdODE). This differential equation system uses the logarithm of the niche-index as the independent variable and models the dynamics of the population proportions in the qdODE framework, rather than the net population counts. This analysis is in direct analogy to the classical work done in evolutionary game theory and its extensions [6–16].

We show that this system of differential equations is closely related to the discrete time replicator equation studied in [7, 12]. In particular we relate asymptotic properties of these equations (in terms of niche index)

---

*Applied Research Laboratory, Penn State University, University Park, PA 16802, USA, E-mail: griffinch@psu.edu

†Beijing Advanced Innovation Center for Tree Breeding by Molecular Design, Center for Computational Biology, College of Biological Sciences and Technology, Beijing Forestry University, Beijing 100083, China, E-mail: libojiang@bjfu.edu.cn

‡Center for Statistical Genetics, Departments of Public Health Sciences and Statistics, The Pennsylvania State University, Hershey, PA 17033, USA, E-mail: RWu@phs.psu.edu

to the Nash equilibria of an underlying game matrix, establishing a simple variant of the folk theorem of evolutionary games [11]. We show that this equation system has special properties for populations playing generalized rock-paper-scissors with homogenous birth/death rates. The main purpose of this paper is to expand on the mathematical properties of qdODE first observed in [1] and relate them to the standard evolutionary game theory literature. We note that evolutionary games are an extremely well studied area in mathematics [9–11], physics [15–18] and biology [14]. Tanimoto [17, 18] and Friedman & Sinervo [14] offer excellent modern treatments on the subject. In the sequel, we also mention the relationship between the generalized rock-paper-scissors dynamic considered in this work and the classic three state Potts model [19–24]. We also note that rock-paper-scissors is commonly studied in evolutionary game theory as an archetypical examples of a three-strategy game [11, 17, 18].

2 Model

We consider a finite population model of n interacting species. Let $X_i(t)$ be the count of species i at time t and suppose that the *niche index* is:

$$M(t) = \sum_i X_i(t). \tag{1}$$

The population proportion is denoted:

$$x_i(t) = \frac{X_i(t)}{M(t)}. \tag{2}$$

Population and proportion vectors are given by:

$$\mathbf{X} = \langle X_1, \dots, X_n \rangle \qquad\qquad \mathbf{x} = \langle x_1, \dots, x_n \rangle .$$

In general, we have $\mathbf{X} \in \mathbb{R}_+$ and $\mathbf{x} \in \Delta_n$, where Δ_n is the $(n-1)$-dimensional unit simplex defined by:

$$\Delta_n = \left\{ \mathbf{x} \in \mathbb{R}^n : \mathbf{1}^T\mathbf{x} = 1 \text{ and } \mathbf{x} \geq 0 \right\}.$$

Here $\mathbf{1}$ is an appropriate dimension vector consisting of all 1's.

Suppose:

$$\dot{\mathbf{X}} = \mathbf{F}(\mathbf{X}, M), \tag{3}$$

here $\mathbf{F} : \mathbb{R}^n \to \mathbb{R}^n$. Then:

$$\dot{M} = \mathbf{1}^T\mathbf{F}(\mathbf{X}, M). \tag{4}$$

Rather than focus on the dynamics of X_i (or x_i) as a function of time, we consider the dynamics of X_i (and x_i) as functions of the total population in order to understand the potential whole-part relationships that may emerge. In particular, we seek to quantify the behavior of dX_i/dM and dx_i/dM rather than $\dot{X}_i$ or $\dot{x}_i$ as in the traditional replicator dynamics.

Given a population vector $\mathbf{X}$ that varies according to Eq. (3), the quasi-dynamic population equation is:

$$\mathbf{X}'(M) = \frac{\mathbf{F}(\mathbf{X}, M)}{\mathbf{1}^T\mathbf{F}(\mathbf{X}, M)}. \tag{5}$$

Understanding quasi-dynamic population equations is critical when there is only a limit sense of common "time" or when only a few samples may be taken limiting time series analysis. Situations like this occur frequently, for example when working with human subjects (i.e., when sampling *in vivo* from human patients).

3 Interactive Growth Model

Assume the underlying (hidden) dynamics are given by:

$$\dot{X}_i = X_i \left(\lambda_i + \mathbf{e}_i^T \mathbf{A}\mathbf{x} \right). \tag{6}$$

Here $\mathbf{A}$ is an interaction (community or game) matrix and λ_i is an intrinsic birth/death rate for species i. This is consistent with the model in [25].

Let $\boldsymbol{\lambda}$ be the vector of population birth/death rates. Applying Eq. (5), we obtain:

$$\frac{dX_i}{dM} = \frac{X_i\left(\lambda_i + \mathbf{e}_i^T\mathbf{A}\mathbf{x}\right)}{\sum_j X_j\left(\lambda_i + \mathbf{e}_j^T\mathbf{A}\mathbf{x}\right)}. \tag{7}$$

Note that:

$$\mathbf{x} = \frac{1}{M}\mathbf{X},$$

and

$$\sum_j X_j\mathbf{e}_j^T\mathbf{A}\mathbf{x} = \mathbf{X}^T\mathbf{A}\mathbf{x} = \frac{1}{M}\mathbf{X}^T\mathbf{A}\mathbf{X}.$$

Using these facts, we can simplify Eq. (7) to obtain the quasi-dynamic population equations:

$$\frac{dX_i}{dM} = \frac{\lambda_i X_i + \frac{X_i}{M}\mathbf{e}_i^T\mathbf{A}\mathbf{X}}{\boldsymbol{\lambda}^T\mathbf{X} + \frac{1}{M}\mathbf{X}^T\mathbf{A}\mathbf{X}}. \tag{8}$$

From this we note that if $\boldsymbol{\lambda} = \mathbf{0}$, then dynamics are autonomous, and given by:

$$\frac{dX_i}{dM} = X_i\frac{\mathbf{e}_i^T\mathbf{A}\mathbf{X}}{\mathbf{X}\mathbf{A}\mathbf{X}}. \tag{9}$$

In the absence of interaction, the dynamics are also autonomous and given:

$$\frac{dX_i}{dM} = \frac{\lambda_i X_i}{\boldsymbol{\lambda}^T\mathbf{X}}. \tag{10}$$

Taken together, however, the qdODE system is a non-autonomous system of differential equations. In the sequel, we will show that the proportional form of these equations can be made naturally autonomous through a change of variables.

3.1 Emergence of Power Scaling Phenomena

The existence of allometric scaling in gene network data is observed in [1]. Here we derive this phenomena for the case of weak interaction and using the point of view of a Walrasian equilibrium in which we assume that each species is a small fraction of the whole microbiome of the organism. In specific, we show that a power scaling law emerges naturally in the case of limited interactions in environments where no species dominates the entire population. This observation is used in [1] as part of their statistical modeling.

Consider a simple case with limited interaction where we are concerned with only one species whose population quantity is given by X_1. All other species are assumed to be grouped together as a second species whose population quantity is given by X_2. From Eq. (10), when $\mathbf{A} \approx \mathbf{0}$ we have the two-dimensional system:

$$\begin{cases} \dfrac{dX_1}{dM} = \dfrac{\lambda_1 X_1}{\lambda_1 X_1 + \lambda_2 X_2} \\ \dfrac{X_2}{dM} = \dfrac{\lambda_2 X_2}{\lambda_1 X_1 + \lambda_2 X_2} \end{cases}. \tag{11}$$

Eq. (11) can be solved exactly by using X_1 as a reference species:

$$\frac{dX_2}{dX_1} = \frac{\lambda_2 X_2}{\lambda_1 X_1}. \tag{12}$$

Integrating the separable system yields:

$$X_2 = \frac{A}{\lambda_2}\left(\lambda_1 X_1\right)^{\frac{\lambda_2}{\lambda_1}}, \tag{13}$$

where A is a constant of integration. Then we compute:

$$M = X_1 + X_2 = X_1 + \frac{A}{\lambda_2}\left(\lambda_1 X_1\right)^{\frac{\lambda_2}{\lambda_1}}. \tag{14}$$

Observe, when $X_1 \ll M$, (as we assumed), then:

$$M \approx \frac{A}{\lambda_2} \left(\lambda_1 X_1\right)^{\frac{\lambda_2}{\lambda_1}}. \tag{15}$$

In this approximation, we can solve for X_1 and observe that:

$$X_1 \approx \frac{1}{\lambda_1} \left(\frac{\lambda_2 M}{A}\right)^{-\frac{\lambda_2}{\lambda_1}}. \tag{16}$$

Thus, when no species dominates and interaction is small, we see that the quantity of each species should behave according to a power law; i.e., the system will exhibit allometric scaling of whole to part.

It is worth asking how $\mathbf{A} \approx \mathbf{0}$ would emerge in a complex system. If we consider the more complex growth model:

$$\dot{X}_i = X_i \left(\left(1 - \frac{M}{M^*}\right)\lambda_i + \frac{M}{M^*}\mathbf{e}_i^T \mathbf{A}\mathbf{x}\right), \tag{17}$$

where M^* is a carrying capacity for the entire ecology, then for $M \ll M^*$, the interaction component is small. Analysis of this more complete model is left to future work in order to study the properties of the simpler model. However we note that empirical evidence supporting the emergence of power-law scaling in naturally occurring microbiota be found in [1].

4 Proportional Quasi-Dynamic ODE

In this section we investigate the properties of the quasi-dynamic ODE for the population proportions x_i (as compared to X_i).

Applying the quotient rule to X_i/M yields:

$$\frac{1}{M}\frac{dX_i}{dM} - \frac{X_i}{M^2} = \frac{1}{M}\left(\frac{\lambda_i X_i + x_i \mathbf{e}_i^T \mathbf{A}\mathbf{X}}{\boldsymbol{\lambda}^T \mathbf{X} + \mathbf{x}\mathbf{A}\mathbf{X}}\right) - \frac{1}{M}x_i,$$

where we replace X_i/M with x_i and $\mathbf{X}/M$ with $\mathbf{x}$. Factoring M out of the top and bottom yields:

$$\frac{dx_i}{dM} = \frac{1}{M}\left(\frac{M}{M} \cdot \frac{\lambda_i x_i + x_i \mathbf{e}_i^T \mathbf{A}\mathbf{x}}{\boldsymbol{\lambda}^T \mathbf{X} + \frac{1}{M}\mathbf{x}\mathbf{A}\mathbf{x}}\right) - \frac{1}{M}x_i.$$

Factoring and simplification yields the proportional quasi-dynamic ODE:

$$\frac{dx_i}{dM} = \frac{x_i}{M}\left(\frac{\lambda_i + \mathbf{e}_i^T \mathbf{A}\mathbf{x}}{\bar{\lambda}(\mathbf{x}) + \mathbf{x}^T \mathbf{A}\mathbf{x}} - 1\right), \tag{18}$$

where:

$$\bar{\lambda}(\mathbf{x}) = \sum_i \lambda_i x_i. \tag{19}$$

Eq. (18) is clearly non-autonomous, but we can analyze an equivalent autonomous system by a simple change of variables. Let $L = \log(M)$. Then we have the following:

$$\frac{dx_i}{dM} = x_i \frac{dL}{dM}\left(\frac{\lambda_i + \mathbf{e}_i^T \mathbf{A}\mathbf{x}}{\bar{\lambda} + \mathbf{x}^T \mathbf{A}\mathbf{x}} - 1\right).$$

This implies:

$$\frac{dx_i}{dL} = x_i\left(\frac{\lambda_i + \mathbf{e}_i^T \mathbf{A}\mathbf{x}}{\bar{\lambda} + \mathbf{x}^T \mathbf{A}\mathbf{x}} - 1\right). \tag{20}$$

We note that these dynamics are a continuous variation of the discrete time replicator dynamics discussed in [7, 12] (see Eq. 2.1 of [7]), where time is replaced by the logarithmic population size and we consider continuous (rather than discrete) change. The fact that the proportional quasi-dynamic ordinary differential equations are related (in form) to the discrete time replicator dynamic is both interesting and useful, since we can use results from classical evolutionary game theory to derive properties of these equations for varying population sizes. For this reason, we refer to Eq. (20) as the *quasi-dynamic replicator equation*.

4.1 Analysis of the Quasi-Dynamic Replicator Equation

Suppose $\lambda_i = 0$ for all i and $\mathbf{x}^*$ is a strict Nash equilibrium. Further assume that $\mathbf{x}^T\mathbf{A}\mathbf{x} > 0$, then as $t \to \infty$ we have $L \to \infty$. In particular from the folk theorem of evolutionary game theory [11], we know that if $\mathbf{x}^*$ is a strict Nash equilibrium, then it is asymptotically stable in the replicator dynamics [11]. Consequently we have shown that there is some neighborhood $\mathcal{N}$ of $\mathbf{x}^*$ in which all trajectories asymptotically approach $\mathbf{x}^*$ as $L \to \infty$.

Despite the relationship to the replicator, the asymptotic behavior of Eq. (20) is distinct from the behavior of the ordinary replicator. To see this, note that the extreme points of the simplex need not be fixed points of the dynamics when $\lambda_i = 0$ for all i.

Moreover, suppose $\mathbf{x}^*$ is a unique globally asymptotically stable fixed point for $\dot{\mathbf{x}}$ and $\dot{L} > 0$ for all $\mathbf{x}$. Then, $\mathbf{x}^*$ is asymptotically stable as $L \to \infty$. On the other hand, if $\mathbf{x}^*$ is a unique globally asymptotically unstable fixed point for $\dot{\mathbf{x}}$ and $\dot{L} < 0$ for all $\mathbf{x}$, then $\mathbf{x}^*$ is (also) asymptotically stable as $L \to \infty$. In essence, by considering population explosion, we are working backward in time, rather than forward in time.

4.2 Illustration of Results

We will illustrate this using the biased rock-paper-scissors matrix:

$$\mathbf{A} = \begin{bmatrix} 0 & -1 & 1+a \\ 1+a & 0 & -1 \\ -1 & 1+a & 0 \end{bmatrix}.$$

We assume $a > -1$, otherwise, the dynamics are no longer rock-paper-scissors. Before proceeding, we note that this matrix can be constructed as a linear combination of a constant (ones) matrix, a traditional rock-paper-scissors matrix as found in [10] and a matrix defining a coordination component (the bias), which is similar to a Potts model [26]. Various combinations of rock-paper-scissors and the Potts model and their relationship have been studied extensively [19–24].

In the ordinary replicator dynamics, the internal fixed point $\mathbf{x}^* = \left\langle \frac{1}{3}, \frac{1}{3}, \frac{1}{3} \right\rangle$ is stable if and only if $a > 0$. However, note that this a fixed point for Eq. (20) only when $a \neq 0$. Moreover, first order analysis yields the eigenvalues of the Jacobian equal to:

$$\{\lambda_1, \lambda_2, \lambda_3\} = \left\{ -1, -\frac{1}{2} - \frac{i|2+a|\sqrt{3}}{2a}, -\frac{1}{2} + \frac{i|2+a|\sqrt{3}}{2a} \right\}. \tag{21}$$

Thus as $L \to \infty$, $\left\langle \frac{1}{3}, \frac{1}{3}, \frac{1}{3} \right\rangle$ is stable as long as $a \in (-1, \infty)$. This is illustrated for $a = -\frac{1}{10}$ in Fig. 1. We note the whip that occurs as $L \to 0$ is a result of the instability of the interior fixed point in the ordinary rock-paper-scissors and the fact that the three simplex extreme points are stable in the ordinary replicator dynamic. Thus for small niche indexes, one should expect numerical instability in any analysis, illustrating a caveat on the use of the quasi dynamic approach.

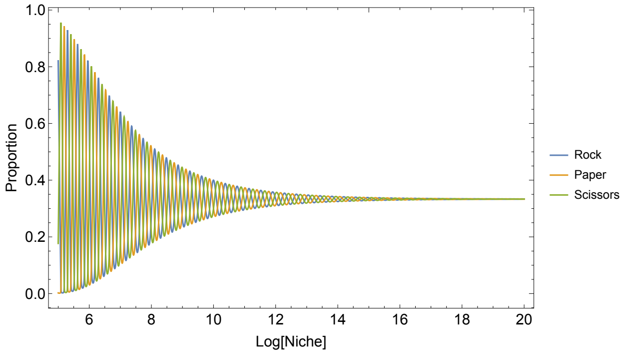

Figure 1: Illustration of the behavior of generalized rock-paper-scissors with negative growth.

5 Detailed Analysis of Rock-Paper-Scissors with Symmetric Populations

Heretofore we have considered the case when $\lambda_i = 0$. We now relax this assumption and conduct an analysis for symmetric populations under varying assumptions and show that the behavior is consistent with the discrete time behavior of rock-paper-scissors [11]. This analysis also serves to illustrate the types of dynamics that might be observed in the wild.

5.1 Case: $a \neq 0$

Assume three species with equal growth rates so that $\lambda_i = \lambda$ for all $i \neq j$. The eigenvalues of the Jacobian matrix about the interior fixed point $\left\langle \frac{1}{3}, \frac{1}{3}, \frac{1}{3} \right\rangle$ are given by:

$$\{\lambda_1, \lambda_2, \lambda_3\} = \left\{ -1, \frac{-a - i|2+a|\sqrt{3}}{2(a+3\lambda)}, \frac{-a + i|2+a|\sqrt{3}}{2(a+3\lambda)} \right\}. \tag{22}$$

Assuming $a > 0$, then when $\lambda < -\frac{a}{3}$, the resulting interior fixed point is unstable. A symmetry argument shows that the eigenvalues of the Jacobian at any of the extreme points of the simplex are:

$$\{\lambda_1, \lambda_2, \lambda_3\} = \left\{ -\frac{1}{\lambda}, \frac{1+a}{\lambda}, -1 \right\}. \tag{23}$$

Thus the extreme points are hyperbolic and unstable when $\lambda < 0$ and $a > -1$. This unnatural situation can be interpreted by noting that:

$$\dot{M} = \left(\lambda M + M \mathbf{x}^T \mathbf{A} \mathbf{x} \right). \tag{24}$$

In particular, when $a > 0$, then $\mathbf{x}^T \mathbf{A} \mathbf{x} \in \left[0, \frac{a}{3}\right]$. Thus,

$$\left(\lambda M + M \mathbf{x}^T \mathbf{A} \mathbf{x} \right) \leq \left(\lambda M + \frac{a}{3} M \right).$$

This implies that

$$\dot{M} \leq \left(\lambda + \frac{a}{3} \right) \leq 0. \tag{25}$$

Thus in this case, the population is monotonically decreasing and the proportions exhibit whip as the population collapses. Conversely, if $a > 0$ and $\lambda > -\frac{a}{3}$, then the population is increasing and will converge in the long-run to the asymptotically stable interior fixed point. This is illustrated in the Fig. 2, where population decrease is illustrated by tracing the trajectory from right to left.

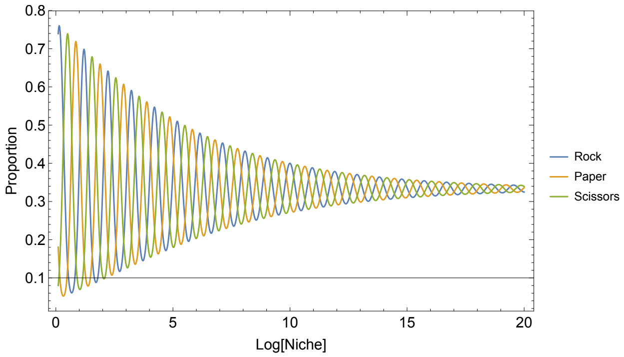

Figure 2: An illustration of equal growth rates in biased rock-paper-scissors with interior fixed point unstable in negative population growth.

5.2 Case $a = 0$

In the case when $a = 0$ and all players are symmetric, the symmetric interior fixed point becomes a non-linear center and the populations oscillate about the interior fixed point for varying log-niche-indexes. To see this, first note that the rock-paper-scissors system can be transformed into a two-dimensional system by setting $x_3 = 1 - x_1 - x_2$. The resulting eigenvalues for the fixed point $x_1 = x_2 = \frac{1}{3}$ are:

$$\lambda_{1,2} = \pm \frac{i}{\sqrt{3}\lambda}. \tag{26}$$

The eigenvalues for the extreme points (single species solutions) are given by:

$$\lambda_{1,2} = \pm \frac{1}{\lambda}. \tag{27}$$

Thus the extreme points are again hyperbolic and unstable. Analysis of the center manifold at the interior fixed point can be accomplished by following the standard analysis used in the ordinary Lotka-Volterra equations. Compute:

$$\frac{dx_2}{dx_1} = \frac{dx_2}{dL}\frac{dL}{dx_1} = -\frac{x_2\left(2x_1 + x_2 - 1\right)}{x_1\left(x_1 + 2x_2 - 1\right)}. \tag{28}$$

This differential equation can be solved explicitly[1] and yields the implicit expression:

$$f(x_1, x_2) = x_1^2 x_2 + x_1 x_2^2 - x_1 x_2 = C, \tag{29}$$

that solutions of Eq. (28) must satisfy. Here C is a constant of integration. It is straightforward to see that:

$$\nabla f\left(\tfrac{1}{3}, \tfrac{1}{3}\right) = 0. \tag{30}$$

Moreover, evaluating the Hessian matrix of f at $x = y = \frac{1}{3}$ yields:

$$\mathbf{H} = \begin{bmatrix} \frac{2}{3} & \frac{1}{3} \\ \frac{1}{3} & \frac{2}{3} \end{bmatrix},$$

which has eigenvalues 1 and $\frac{1}{3}$. Thus, the Hessian matrix is positive semi-definite and $x_1 = x_2 = \frac{1}{3}$ must be a local-minimum for f. This implies that in a neighborhood of the fixed point, the solution curves of the proportional qdODE must be closed and thus the fixed point is a center. This is illustrated in Fig. 3, where we show a vector field plot with a clear non-linear center and solution plots for $\lambda = \frac{1}{10}$. It is worth noting (as before) that the sign of λ does not affect the solution curves, but impacts the direction along the log-niche-index axis the system should be considered evolving.

5.3 General Behaviors of qdODE

In general, it is worth noting that the proportional quasi-ODE dynamics can exhibit a large variety of behaviors. We illustrate this in Fig. 4 using $a = -\frac{1}{10}$ in the biased rock-paper-scissors matrix and $\lambda_1 = 0.3$, $\lambda_2 = 0.4$ and $\lambda_3 = 0.9$ with starting state $x_1(10) = 0.4$, $x_2(10) = 0.3$ and $x_3(10) = 0.3$. Notice that the proportions oscillate as a result of the cyclic interactions defined by $\mathbf{A}$ but mediated by endogenous growth from the unbalanced growth rates. Constructing a complete theory for asymmetric populations is left as future work.

6 Conclusions

In this paper, we studied a mathematical formulation of the quasi-dynamic ordinary differential equations first defined empirically in [1]. We showed that simple non-linear qdODE systems arise when the temporal dynamics governing a (difficult to sample) population are given by the generalized Lotka-Volterra equations.

---

[1] Mathematica provides an automatic solution.

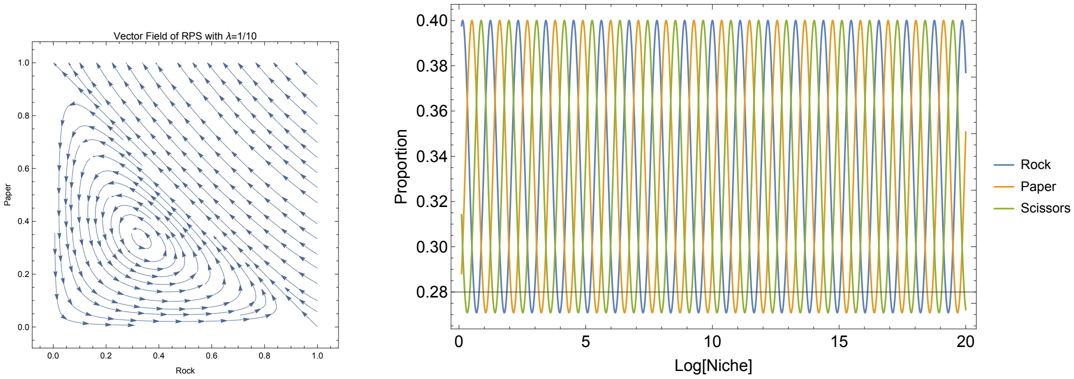

(a) 2D Vector Field Plot

(b) Solution Curves

Figure 3: (a) The two-dimensional vector field plot of the dynamics of rock and paper (scissors is linearly dependent on these values). The vector field clearly indicates the presence of a center. (b) Solution curves for the qdODE with ordinary rock-paper-scissors and a symmetric growth rate of $\lambda = \frac{1}{10}$.

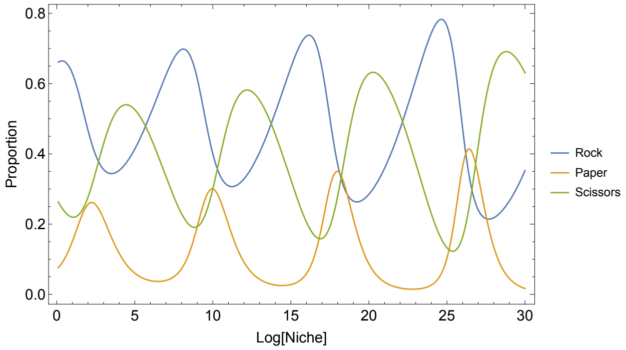

Figure 4: An illustration of the behavior of the proportional quasi-dynamic ODE system using asymmetric parameters.

We showed how allometric scaling arises naturally from these dynamics under a weak interaction assumption, thus providing a mathematical explanation for the empirical observation in [1]. We then studied the proportional qdODE and showed that under a non-linear transformation of niche-index to log-niche-index an autonomous non-linear system emerges that has properties similar to the ordinary replicator and is (in fact) the continuous analog of the discrete replicator dynamic studied in [7, 12]. We showed formal properties of this system and studied the case of a symmetric population playing using generalized Lotka-Volterra dynamics with a biased rock-paper-scissors interaction matrix.

In future work, we will study the theoretical properties of asymmetric populations further and determine their behavior under changing niche index. Additionally, it may be instructive to analyze the model given in Eq. (17). Cursory analysis shows that the proportional form of this equation is non-autonomous (in $\log(M)$) making analysis more complex, but potentially more interesting. As additional future work, it may also be possible to consider more general interaction dynamics that include population specific carrying capacities. Extending [1] and studying the relationship of these mathematical models with real-world data is also a future priority.

Acknowledgement

Portions of CG's work were supported in part by the National Science Foundation Grant DMS-1814876. LJ was supported by the Fundamental Research Funds for the Central Universities (NO. 2015ZCQ-SW-06, NO. BLX2015-23), grant 31700576 from National Natural Science Foundation of China, grant 31600536 from National Natural Science Foundation of China, and grant 201404102 from the State Administration of Forestry of China.

References

[1] C. Chen, L. Jiang, G. Fu, M. Wang, Y. Wang, B. Shen, Z. Liu, Z. Wang, W. Hou, S. A. Berceli, and R. Wu, "An omnidirectional visualization model of personalized gene regulatory networks," *npj Systems Biology and Applications*, vol. 5, no. 1, p. 38, 2019. [Online]. Available: https://doi.org/10.1038/s41540-019-0116-1

[2] K. Finlay and G. Wilkinson, "The analysis of adaptation in a plant-breeding programme," *Australian journal of agricultural research*, vol. 14, no. 6, pp. 742–754, 1963.

[3] C. S. Elton, *Animal ecology.* University of Chicago Press, 2001.

[4] C. Hui, "Carrying capacity, population equilibrium, and environment's maximal load," *Ecological Modelling*, vol. 192, no. 1-2, pp. 317–320, 2006.

[5] F. C. Pereira and D. Berry, "Microbial nutrient niches in the gut," *Environmental microbiology*, vol. 19, no. 4, pp. 1366–1378, 2017.

[6] P. D. Taylor and L. B. Jonker, "Evolutionarily stable strategies and game dynamics," *Mathematical biosciences*, vol. 40, no. 1-2, pp. 145–156, 1978.

[7] J. Hofbauer, "A difference equation model for the hypercycle," *SIAM Journal on Applied Mathematics*, vol. 44, no. 4, pp. 762–772, 1984.

[8] K. Sigmund, "A survey of replicator equations," in *Complexity, Language, and Life: Mathematical Approaches.* Springer, 1986, pp. 88–104.

[9] J. Hofbauer and K. Sigmund, *Evolutionary Games and Population Dynamics.* Cambridge University Press, 1998.

[10] J. W. Weibull, *Evolutionary Game Theory.* MIT Press, 1997.

[11] J. Hofbauer and K. Sigmund, "Evolutionary Game Dynamics," *Bulletin of the American Mathematical Society*, vol. 40, no. 4, pp. 479–519, 2003.

[12] J. Alboszta, J. Mie *et al.*, "Stability of evolutionarily stable strategies in discrete replicator dynamics with time delay," *Journal of theoretical biology*, vol. 231, no. 2, pp. 175–179, 2004.

[13] D. F. Toupo and S. H. Strogatz, "Nonlinear dynamics of the rock-paper-scissors game with mutations," *Physical Review E*, vol. 91, no. 5, p. 052907, 2015.

[14] D. Friedman and B. Sinervo, *Evolutionary games in natural, social, and virtual worlds.* Oxford University Press, 2016.

[15] G. B. Ermentrout, C. Griffin, and A. Belmonte, "Transition matrix model for evolutionary game dynamics," *Phys. Rev. E*, vol. 93, p. 032138, Mar 2016. [Online]. Available: http://link.aps.org/doi/10.1103/PhysRevE.93.032138

[16] C. Griffin and A. Belmonte, "Cyclic public goods games: Compensated coexistence among mutual cheaters stabilized by optimized penalty taxation," *Physical Review E*, vol. 95, no. 5, p. 052309, 2017.

[17] J. Tanimoto, *Fundamentals of evolutionary game theory and its applications.* Springer, 2015.

[18] ——, *Evolutionary Games With Sociophysics.* Springer, 2019.

[19] A. Szolnoki, G. Szabó, and M. Ravasz, "Three-state potts model in combination with the rock-scissors-paper game," *Physical Review E*, vol. 71, no. 2, p. 027102, 2005.

[20] G. Szabó and A. Szolnoki, "Three-state cyclic voter model extended with potts energy," *Physical Review E*, vol. 65, no. 3, p. 036115, 2002.

[21] G. Szabó and T. Czárán, "Phase transition in a spatial lotka-volterra model," *Physical Review E*, vol. 63, no. 6, p. 061904, 2001.

[22] G. Szabó, K. S. Bodó, B. Allen, and M. A. Nowak, "Fourier decomposition of payoff matrix for symmetric three-strategy games," *Physical Review E*, vol. 90, no. 4, p. 042811, 2014.

[23] ——, "Four classes of interactions for evolutionary games," *Physical Review E*, vol. 92, no. 2, p. 022820, 2015.

[24] K. Hódsági and G. Szabó, "Bursts in three-strategy evolutionary ordinal potential games on a square lattice," *Physica A: Statistical Mechanics and its Applications*, vol. 525, pp. 1379–1387, 2019.

[25] E. Paulson and C. Griffin, "Cooperation can emerge in prisoner's dilemma from a multi-species predator prey replicator dynamic," *Mathematical biosciences*, vol. 278, pp. 56–62, 2016.

[26] F.-Y. Wu, "The potts model," *Reviews of modern physics*, vol. 54, no. 1, p. 235, 1982.